A New High-Power Klystron for the DSN

A. Goldfinger
Varian Associates, Inc.

M. A. Gregg and R. Hartop
Radio Frequency and Microwave Subsystems Section

In order to obtain a very-high-reliability 100-kW CW klystron for the DSN high-power transmitters in support of spacecraft to the distant planets, a study contract was awarded to Varian Associates in 1977. Results of that study have been reported previously. This report continues with the last phases of the contract, which resulted in the delivery of a prototype klystron meeting all requirements.

I. Introduction

In 1977, JPL initiated a study program with Varian Associates, Palo Alto, to develop an improved, high-reliability 100-kW CW klystron for the DSN. The program was divided into four phases:

Phase I	Study Definition
Phase II	Design Improvement
Phase III	Electron Gun Fabrication and Evaluation
Phase IV	Prototype Klystron Fabrication and Delivery

The results of Phases I and II were reported in DSN Progress Report 42-50 (pp. 196-205). Phases III and IV are now complete and the results are presented here. Included are data measured on the prototype klystron which met or exceeded all requirements.

II. Electron Gun Fabrication and Beam Analyzer Evaluation

A. Background and New Information

At the conclusion of the Phase II study, it was clear that removal of the modulating anode from the existing X-3060 design klystron would substantially reduce the voltage gradients within the electron gun structure and thereby reduce any tendency toward arcing during high-voltage operation. Computer design techniques were used to modify the focus electrode and anode design to compensate for the removal of the modulating anode. The correct electron trajectories and electron beam size were provided by this computer design.

A logical progression would dictate that the computer design be evaluated in the Varian beam analyzer to verify its performance. However, coincident with the Phase II study, another very-high-power development program (VKS-8269; 450 kW CW @ 2450 MHz) had produced an electron gun with such excellent performance that the decision was made to scale this newly proven design to fit the new VKS-8274 JPL klystron and test this scaled model in the beam analyzer. Beam analyzer testing at this point would be used then to verify the performance of the scaled model as opposed to the more common usage of iterative correction to the Phase II computer design.

This new scaled structure was first evaluated to see that the voltage gradient improvement established in the Phase II computer design would not be compromised. Quite the opposite was true. Because of the new design's larger physical dimensions and more generously radiused electrodes, a significant gain was made. When compared to the Phase II computer design, the highest gradient was reduced by 81%. Compared to the original X-3060's highest gradient of 312 kV/inch, the new design's highest gradient of 143 kV/inch represents an improvement of 312/143 = 2.18X.

Figure 1 presents a comparison of the three designs under discussion. The 250-kW/inch reference line shown represents a generally accepted value for conservative gradient design in a dc application. By any standards, the new VKS-8274 JPL design can be considered ultraconservative.

One additional gain has been made in adopting the new design. Although the new design was scaled "down" from the 450-kW VKS-8269, it represents a scale "up" from the Phase II computer design and the X-3060 structure. The new cathode diameter is 1.263 inches compared to the 1.0-inch diameter of both the X-3060 and Phase II computer design. The increased diameter represents an increased area of 1.595 times and reduces the already conservative cathode loading of 1.375 A/cm^2 to 0.862 A/cm^2. The 0.862 A/cm^2 cathode loading is also in the ultraconservative region, permitting operation of the cathode at reduced temperatures and providing long life reliability.

B. Fabrication Details

To take full advantage of both the electrostatic and magnetic beam analyzer, two versions of the new electron gun were fabricated. The two guns used many common parts, but were different in that one version used no magnetic components whatsoever, and the other used the proposed magnetic pole piece and magnetic field shaping cylinder. The construction of these two models is shown diagrammatically in Figs. 2 and 3.

C. Beam Analyzer Results

The three major goals in the development of an electron gun for the VKS-8274 JPL are (1) correct design perveance, (2) correct design size electron beam, and (3) minimum longitudinal scalloping in the presence of the design magnetic field.

(1) The rf design of the VKS-8274 JPL was established around a perveance 1.0 $\times$ 10^{-6} electron gun. This perveance assures compatibility with existing X-3060 installations and represents a conservative value in terms of good klystron performance and electron optics.

(2) The desired beam size is determined primarily by the rf design parameters. The filling factor (beam size/tunnel size) is a compromise between the desire to have the best coupling (largest beam) for high efficiency and the requirement that the beam be small enough so that interception by the drift tubes will be minimal, thus insuring thermal stability and reliability. Experience has shown that a filling factor of 65% is a desirable compromise. The design tunnel size for the VKS-8274 JPL is 0.480 in.; therefore, the target beam size is 0.65 in. $\times$ 0.480 in. = 0.312 in.

(3) Minimum beam scalloping (size change) is an obvious design requirement, for without a consistent beam size, consistent performance is not possible. A badly scalloping beam will change size markedly with variations in both beam voltage and magnetic field, with subsequent changes in power output, gain and phase response. A reasonable target value for beam scallop is less than 10%, the scallop percentage being defined by:

$$\frac{\text{Beam maximum} - \text{Beam minimum}}{\text{Beam maximum} + \text{Beam minimum}} \times 100.$$

1. Electrostatic test. Testing of any new electron gun design is performed first in the electrostatic beam analyzer to determine its true characteristics without the presence of magnetic fields. Figure 4 shows the electrostatic beam profile in the region of the beam minimum. The region beyond the beam minimum is of no importance in this test since it will later be completely controlled by the confining magnetic field. The beam is cross-sectionally scanned every 0.050 in. from just below the gun anode (0.025 in.) to a point 0.700 in. from the anode. The beam minimum can be seen at a point 0.400 in. from the anode and shows a beam diameter on paper of 0.370 in. The presented curves are always in error (too wide) by the diameter of the pinhole in the scanning target. In this case, the target pinhole is 0.010 in. and when subtracted from the apparent width of 0.370 in. gives a true beam diameter of 0.360 in. This 0.360 in. beam, just 15% larger than the target value of 0.312 in., is considered very suitable for further testing in the magnetic field without alteration of the gun electrodes.

In addition, from the data presented, an excellent beam profile can be seen. The perveance is also on target at 1.008 $\times$ 10^{-6}.

2. Magnetic test. After the electrostatic test above was completed, the electron gun was disassembled and rebuilt to include the magnetic elements. It was then installed in the magnetic beam analyzer for vacuum processing and testing.

Figure 5 shows the beam profile in the presence of all the magnetic elements of the electron gun and operating in the design magnetic field. As in the electrostatic tests, the beam profiles are taken from just below the anode (0.050 in.). In the magnetic tester, however, profiles are taken over an extended range, in this case, 3.5 in., to view more critically the confining effect of the magnetic field. This 3.5 in. scan (not shown) represents a distance in the actual klystron which extends well past the input cavity of the klystron. From this point on, the confining magnetic field is uniform and no further change in the beam profile will occur.

Results of the magnetic beam tester are as follows:

(1) The diameter of the electron beam at the former beam minimum ($Z = 0.400$ in.) has been compressed from 0.360 in. to 0.305 in.).

(2) The first inward scallop occurs at $Z = 1.0$ in. and the beam diameter is measured at 0.280 in.

(3) The first outward scallop occurs at $Z = 1.9$ in. and measured 0.300 in.

(4) The scallop pattern is essentially repeated for the remainder of the Z axis traverse.

Comparison of the largest beam diameter to the design target = 0.312 in./0.300 in. = 1.04 in., just 4% from the design goal.

The beam scallop as defined by

$$\frac{\text{Beam maximum} - \text{Beam minimum}}{\text{Beam maximum} + \text{Beam minimum}} \times 100\%$$

calculates to be:

$$\frac{0.300 - 0.280}{0.300 + 0.280} \times 100\% = 3.45\%, \text{ an insignificant ripple.}$$

The current density profile is quite uniform and compares favorably with well-tested electron beams. The minor variations in the beam profiles, as they are scanned on the Z axis, have been previously traced to slight misalignment of the electron and magnetic axis. This is not expected in the actual klystron.

In summary, the beam analyzer tests have shown the production of an excellent electron optical system, and verify that the excellent performance of VKS-8269 (450 kW @ 2450 MHz) is to a large degree dependent on an excellent electron beam. It permits the prediction of comparable performance in the VKS-8274 JPL.

III. Klystron Prototype Fabrication

A. Mechanical Design Improvements

With only one minor exception, all mechanical improvements proposed in the Phase II Design Improvement final report were incorporated in the VKS-8274 JPL klystron. That one minor exception concerned the lengthening of the electron gun insulator to permit operation of the VKS-8274 JPL in air. This suggestion was found unacceptable with regard to operational safety, and therefore this modification was not incorporated. The insulator's length was changed to permit compatibility with existing oil-filled socket tanks.

The mechanical improvements proposed by the Phase II Design Improvements final report and also incorporated in the VKS-8274 JPL prototype klystron are reviewed below.

1. **Diaphragm trim tuner.** The proposed trim tuner used in the VKS-8274 JPL, and the wide-range tuner now used in the X-3060, are shown in Fig. 6. Casual observation will show the complexity of the old tuner design as compared to the new trim tuner. Not so obvious in the old design are the six vacuum-to-water and three vacuum-to-air brazing joints used in the present X-3060 tuner. In addition to the large number, many of the brazing joints are blind; that is, they can neither be inspected nor repaired after the final braze pass. This type of assembly severely compromises reliability and rebuildability. Compared to this, the trim-tuner design has only *two* vacuum-to-air brazing joints and *no* vacuum-to-water joints. Neither of the vacuum-to-air joints is blind, and both are easily repairable.

In addition to these mechanical advantages, the trim-tuner diaphragm is relatively far removed from the high rf fields at the drift tube gap center and is subjected to far less rf heating than the present X-3060 capacitive paddle. The diaphragm is thermally coupled by large cross-sectional areas of copper to the massive water-cooled copper cavity walls. In Fig. 6, a water-cooled post is shown joined to the diaphragm face. This was a contingency plan only; no diaphragm cooling was required.

2. **Extended tail pipe elimination.** The extended tail pipe configuration shown in Fig. 7 was first introduced in the X-3060 klystron in 1965. Its purpose was to minimize the asymmetry normally caused by the exit path of the output waveguide through the focusing magnet, and to reduce to an absolute minimum body current interception caused by the magnetic asymmetry. Mechanical considerations, however, created an extended tail pipe section that is exposed to a rapidly expanding electron beam just beyond the output gap. This extended section has created both directly and indirectly related failures in the X-3060 klystron. The problem is caused by the fact that the electron beam expands in that region faster than was predicted at the time of the design's introduction, and, in addition, secondary electrons return from the collector to impinge on the tail pipe surfaces. For these reasons, and because the tail pipe is electrically part of the

klystron body, the body current readings for the X-3060 have been recorded as high as 10% of the total beam current (700 mA). This tail pipe current (reading as body current) completely masks body current interception in any other part of the rf structure and is unacceptable because it requires that body current protective-circuit trip levels be set too high (1.0 A). This removes the protection required in the remainder of the rf structure, which may suffer damage from relatively low-quantity (0.050 A), but high-velocity electrons.

Under the circumstances just described, protection *cannot* be provided for the following common field conditions:

(1) Low or incorrectly adjusted magnetic field,

(2) Incorrect tuning,

(3) Overdrive,

(4) Stray magnetic fields (gun region),

(5) Disturbance of the main magnetic field by accidental introduction of ferrous materials (screwdrivers, wrenches, etc.).

Elimination of the extended tail pipe design was a mandatory condition for reliability. Figure 8 shows the new design to be employed in the VKS-8274 JPL klystrons. As shown, the new design provides adequate clearance for the expanding beam and transfers tail pipe interception current to the collector where it is properly metered as collector current. With this configuration, body current readings will return to normal values in the order of 0.050 A, and the rf structure can be properly protected with body current protective trips set at 0.100 A.

One additional design change has been made in conjunction with the elimination of the extended tail pipe. A reentrant output pole piece has been introduced to create a peak in the magnetic field near the output gap. Recent designs have shown that this peaked magnetic field is very beneficial in terms of reducing beam interception in the output region of the klystron. This reentrant design is shown in Fig. 8.

3. Cavity/body construction. During the Phase I investigation of the X-3060, it was found that the rigidity of the rf structure was somewhat lacking, and structural stiffeners were promised for proposed new designs. That is the case, but in addition, recent tests of an X-3060 (May 1978) showed thermal drift attributable to cavity detuning, indicating a need for additional cavity cooling.

The newly designed VKS-8274 JPL incorporates relatively massive copper cavities which have a wall thickness in the order of three times the wall thickness of the present X-3060. Not only does this create a much more rugged rf structure, it permits the passage of water through the cavity walls to insure greater thermal stability. Comparative views of the X-3060 cavity structures and the new design are shown in Figs. 9 and 10. In addition to increased cavity wall thickness and cooling, cavity and walls and drift tubes have increased thermal cross section to provide the best possible thermal stability. This can be seen clearly in Figs. 10 and 11.

In short, the new rf structure has construction closely paralleling a 450-kW klystron (VKS-8270) known to be operationally stable at an even higher frequency; i.e., 2380 MHz.

B. Electrical Design Improvements

Without exception, all electrical design improvements proposed in the Phase II Design Improvement final report were incorporated in the VKS-8274 JPL. Those design improvements are reviewed below.

1. Electron gun redesign. Findings in the Phase II Design Improvement study showed that a substantial improvement could be made in electron gun voltage gradients by removing the modulating anode. This change, plus incorporation of a new optical design, have been incorporated and successfully tested in the VKS-8274 JPL. The improvements and results are fully discussed in Sections I and II.

2. RF structure redesign. During the Phase I investigation of the present X-3060 rf design, a number of deficiencies were noted. These deficiencies were a natural result of designing a klystron with a wide tuning range; i.e., 2114 to 2388 MHz. In particular, drift tube gap spacing and gap-to-gap drift tube distances were compromised to satisfy operation at both ends of the frequency tuning range. In fact, the output cavity drift tube gap in the present X-3060 design is far too long to provide optimum efficiency at either 2114 or 2388 MHz, but it was designed that way to provide low gap capacitance, a requirement of wide tuning range cavities. It was suggested in the Phase II final report that the wide tuning range requirement be eliminated and that two tubes be developed, each electrically optimized for its particular frequency, one at 2114 MHz and the other at 2388 MHz. These tubes would have narrow-range trim tuners only, to permit initial factory tune-up.

JPL's decision at the conclusion of the Phase II final report was to proceed with the development of an optimized design at 2114 MHz. The design chosen and implemented in the VKS-8274 JPL is nearly electrically identical to the 5K70SG klystron. The 5K70SG was used as the basic model because it has demonstrated high efficiency performance, with reliability in numerous field applications for a period exceeding ten years.

The test results shown in Figs. 11-13 and Tables 1 and 2 verify the validity of this approach. Substantial gains were made in efficiency, gain, and bandwidth.

IV. Conclusion

The development of a new high power klystron for the DSN has been very successful as demonstrated by the prototype results. A new contract for four production klystrons has been awarded to Varian Associates, with deliveries planned for early 1983.

Table 1. Certified test report VKS-8274 klystron

	Broad band tuned at 2114 MHz
Power output	146 kW
Beam voltage	37 kV dc
Beam current	7.44 A dc
Beam power input	275 kW
Efficiency	53%
Drive power	0.15 W
Gain	59.8 dB
Bandwidth (– dB)	1.9 MHz
Body current, no rf drive	6.5 MA dc
Body current, sat. rf drive	14 mA dc
Focusing magnet current	12 A dc
Focusing magnet voltage	120 V dc
Heater voltage	10.5 V ac
Heater current	11.35 A ac
Coolant water	
Collector	
Flow	65 gpm
Pressure drop	32 psi
Body	
Flow	7 gpm
Pressure drop	65 psi
Electro-magnet	
Flow	2.5 gpm
Pressure drop	67 psi

Table 2. Comparative data

Parameter	Units	X-3060 performance data	Phase II improvement predictions	VKS-8274 JPL performance data	JPL specification requirements
Frequency	MHz	2114	2114	2114	2114
Beam voltage	kV	36.0	36.0	36.0	40 max
Beam current	Adc	7.7	6.96	7.15	10 max
Power output	kW CW	112.0	132.0	146.0[a]	110 min
Efficiency	%	40.4	52.7	52.8[a]	40 min
Saturation gain	dB	54.7	59.3	59.2	50 min
Saturation BW	MHz	10.4	16.7	18.9[a]	14 min
Body current no rf	MA dc	30.0	–	6.1[a]	–
Body current sat. rf	MA dc	540.0	50.75	11.1[a]	100 max
Electron gun high voltage gradients (worst case)	kV/inch	312.0	254.0	143.0[a]	–
Cathode loading	amps/cm^2	1.375	1.375	0.862[a]	–

[a]Notable improvement over X-3060 performance.

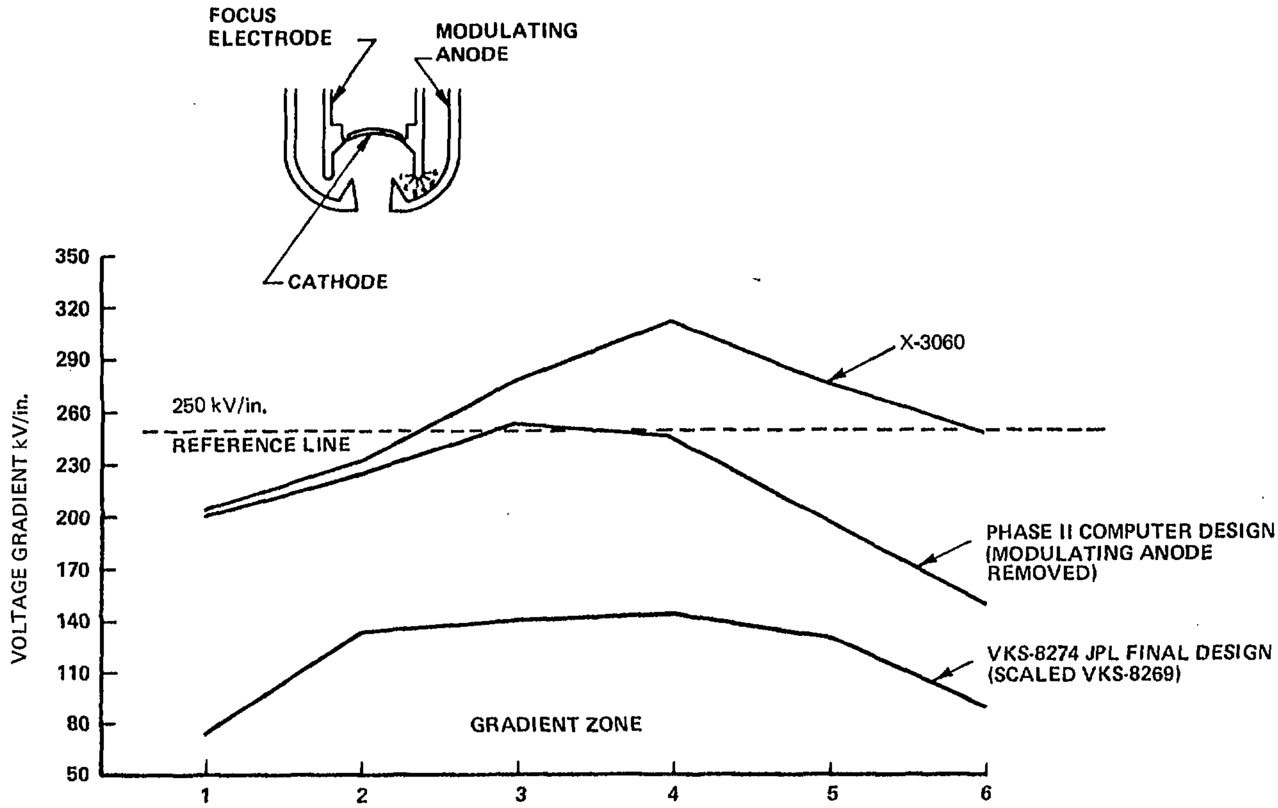

Fig. 1. High voltage gradient comparison: three designs

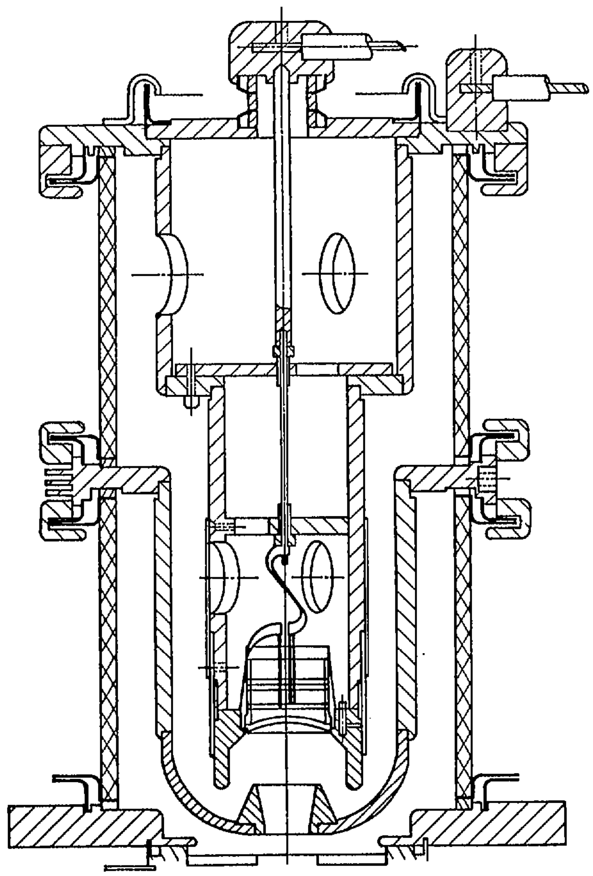

Fig. 2. X-3060 electron gun layout

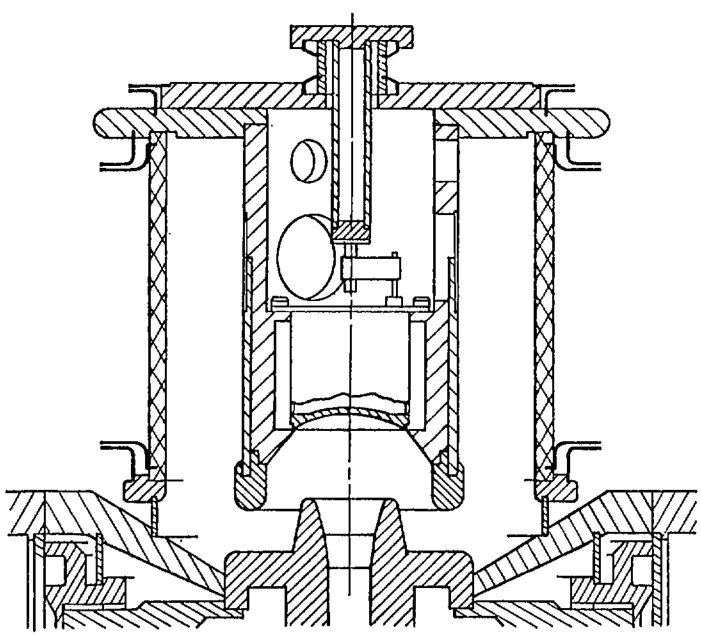

Fig. 3. New design layout VKS-8274 JPL

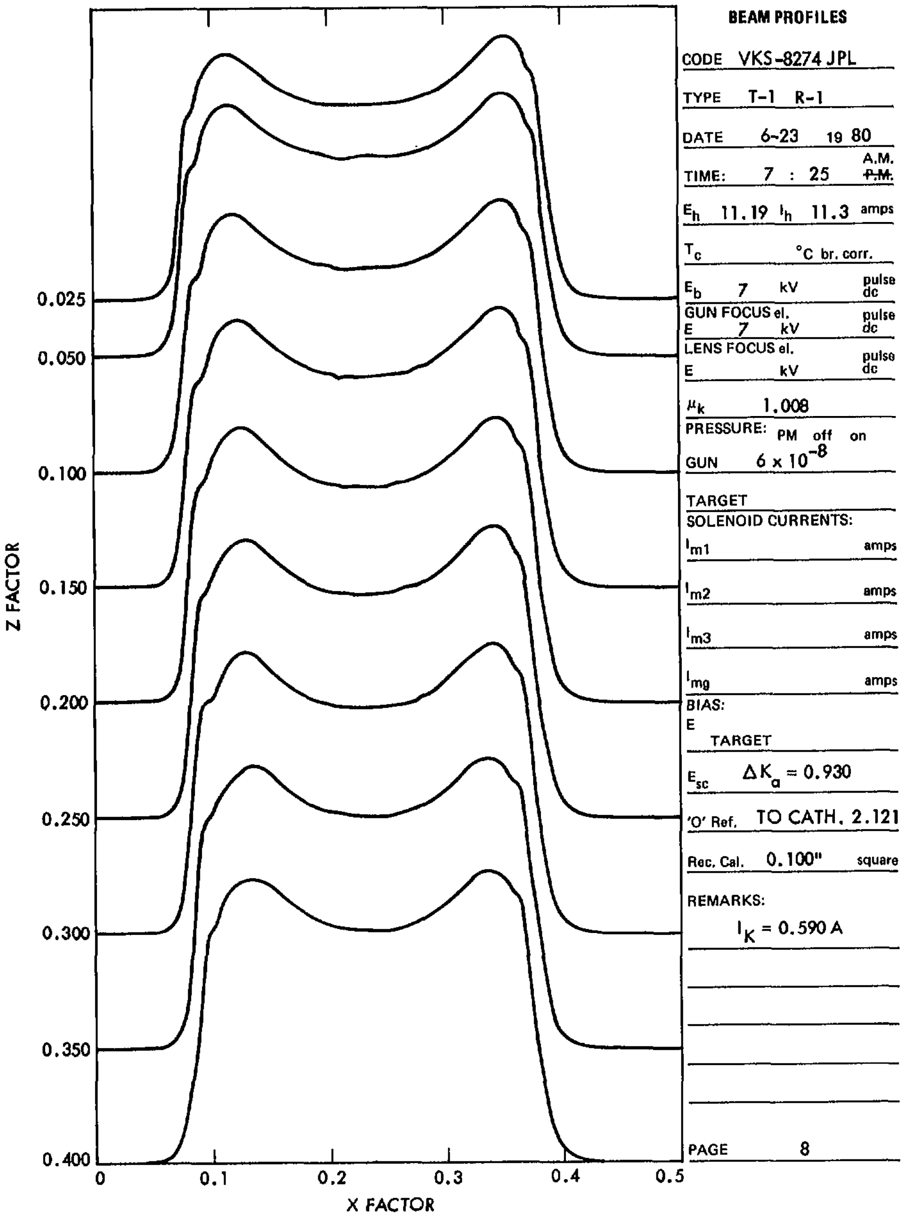

Fig. 4. Electrostatic beam profiles

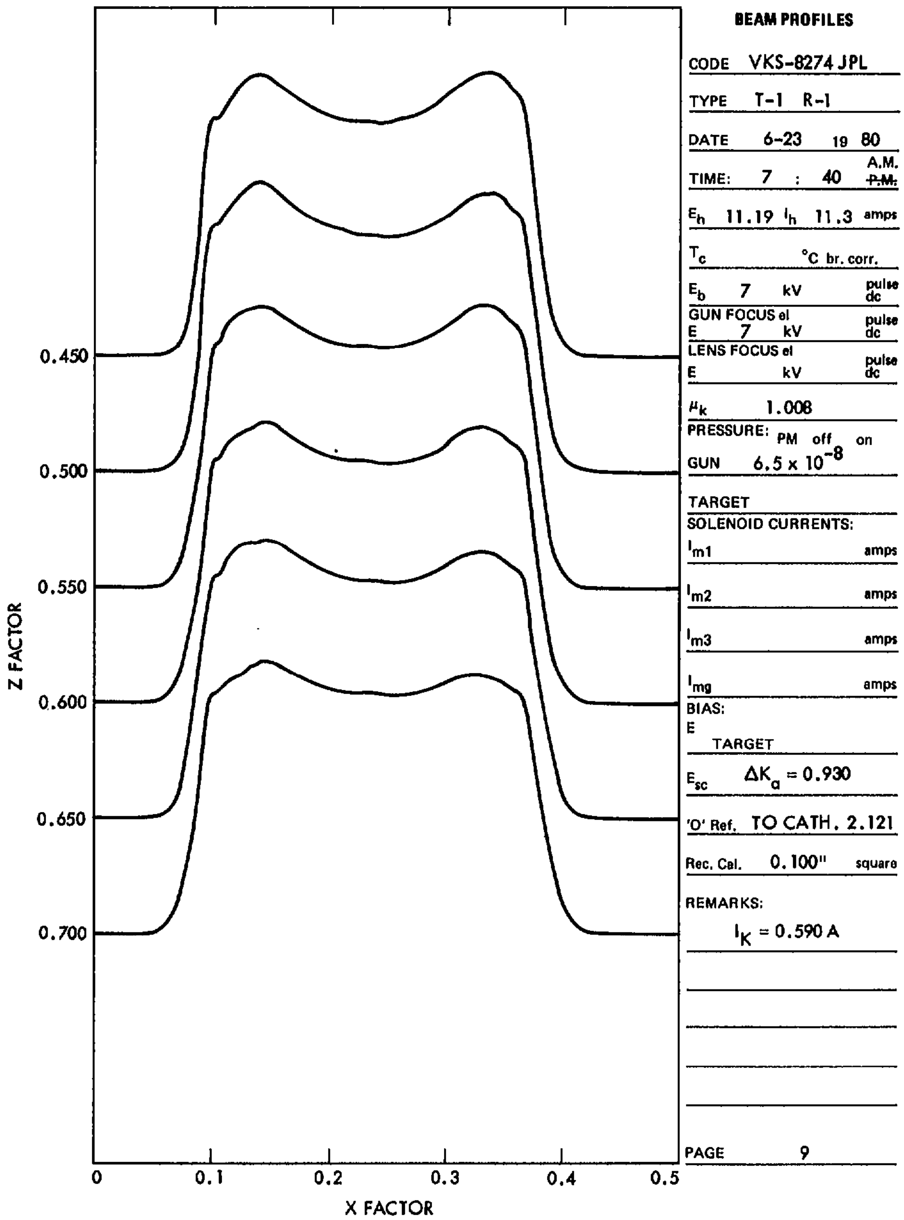
BEAM PROFILES
CODE VKS-8274 JPL
TYPE T-1 R-1
DATE 6-23 19 80
TIME: 7 : 40 A.M. ~~P.M.~~
E h 11.19 I h 11.3 amps
T c °C br. corr.
E b 7 kV pulse dc
GUN FOCUS el E 7 kV pulse dc
LENS FOCUS el E kV pulse dc
μk 1.008
PRESSURE: PM off on
GUN 6.5 x 10-8
TARGET
SOLENOID CURRENTS:
I m1 amps
I m2 amps
I m3 amps
I mg amps
BIAS: E TARGET
E sc ΔK a = 0.930
'0' Ref. TO CATH. 2.121
Rec. Cal. 0.100" square
REMARKS:
I K = 0.590 A
PAGE 9
0.450
0.500
0.550
0.600
0.650
0.700
Z FACTOR
0
0.1
0.2
0.3
0.4
0.5
X FACTOR

Fig. 4 (contd)

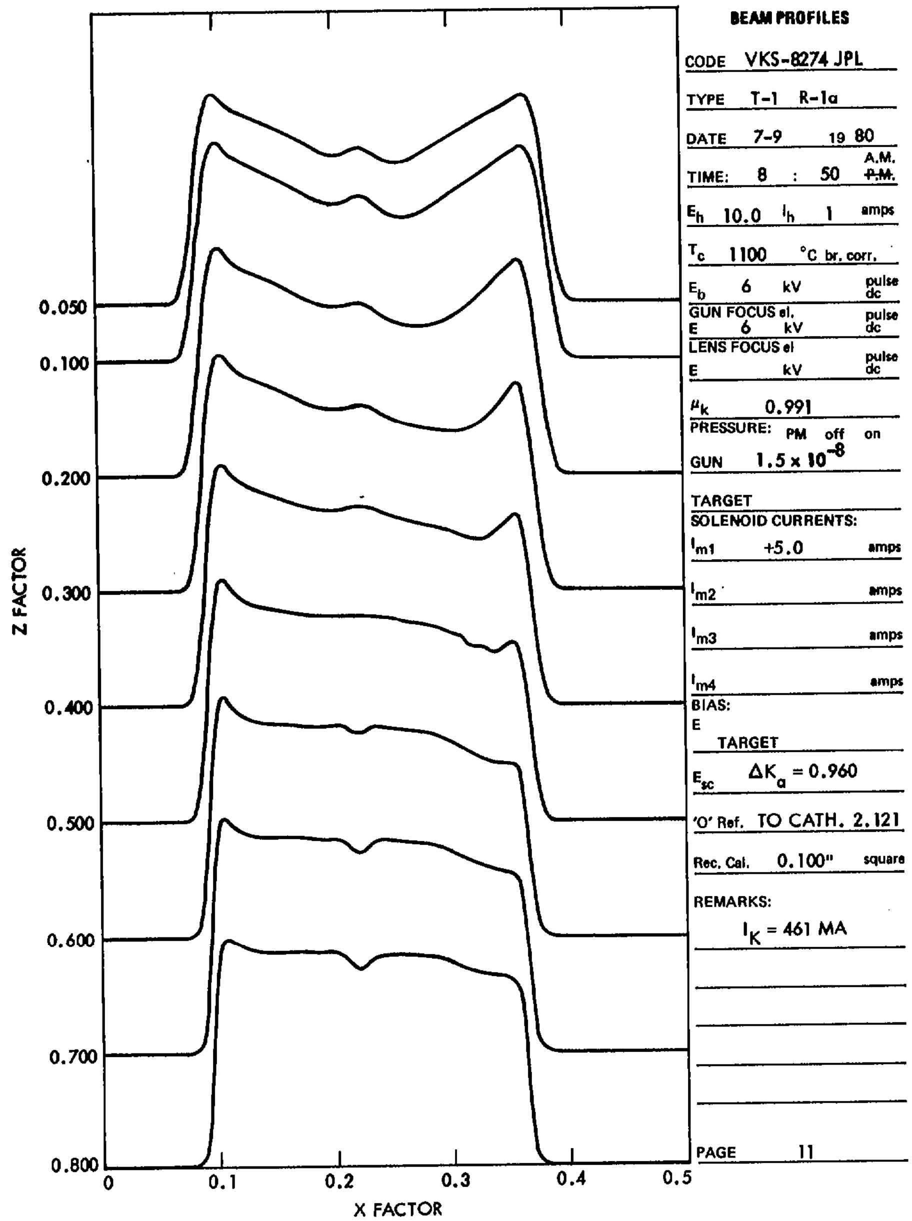

Fig. 5. Magnetic beam profiles

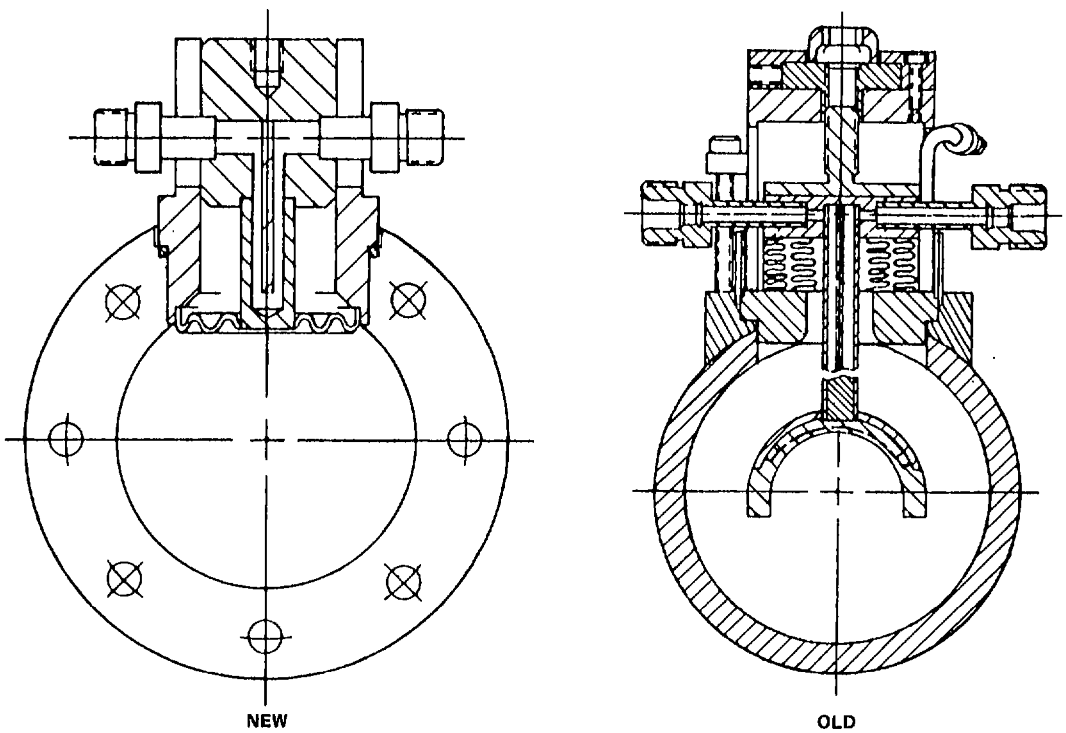

Fig. 6. Tuner designs compared

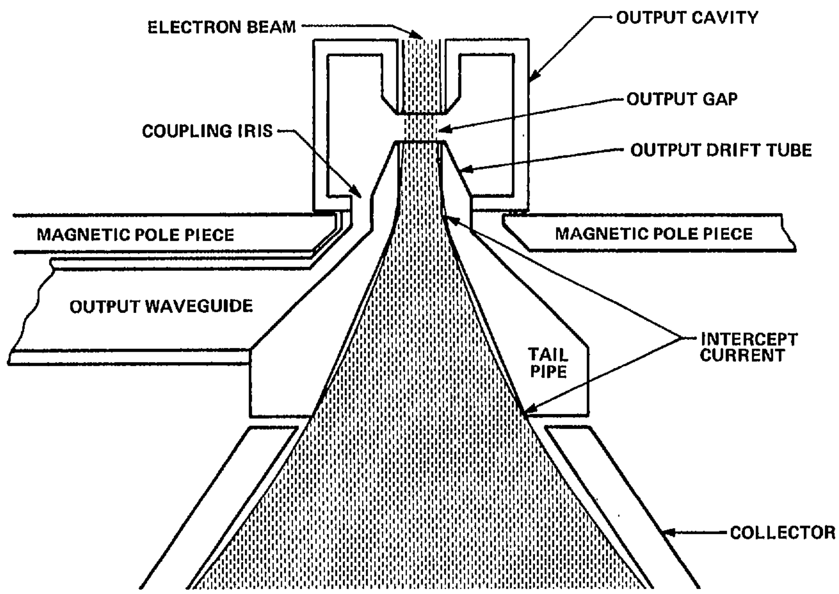

Fig. 7. X-3060 extended tail pipe

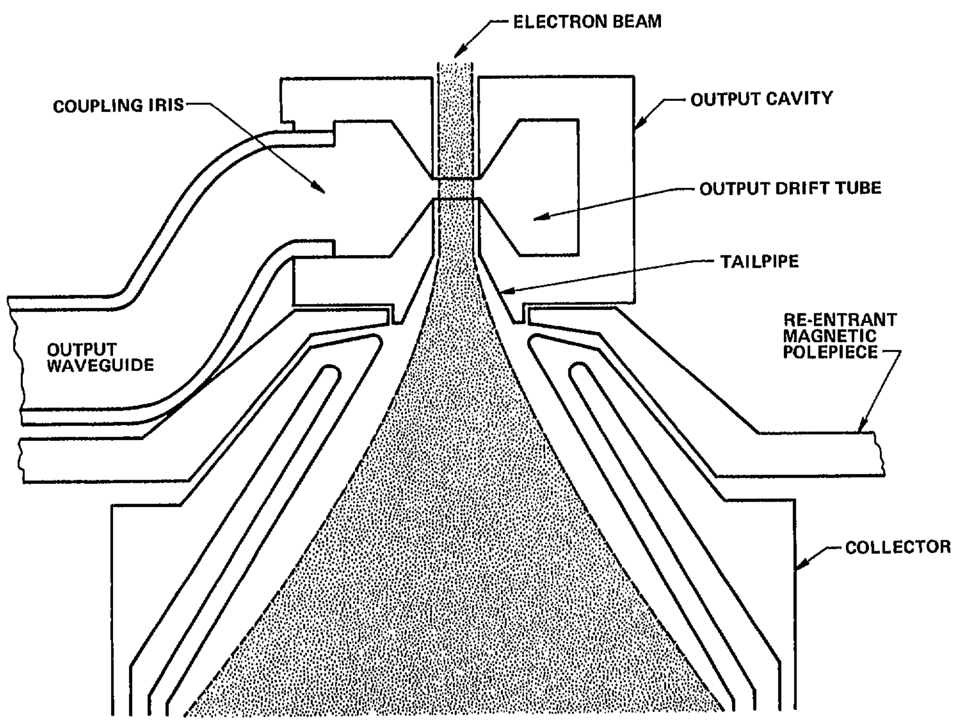

Fig. 8. VKS-8274 JPL output circuit

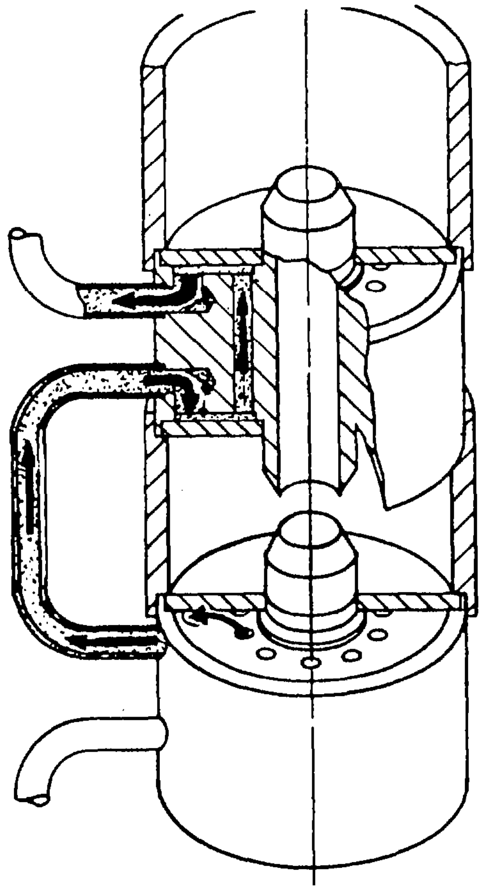

Fig. 9. Old cavity structure (X-3060)

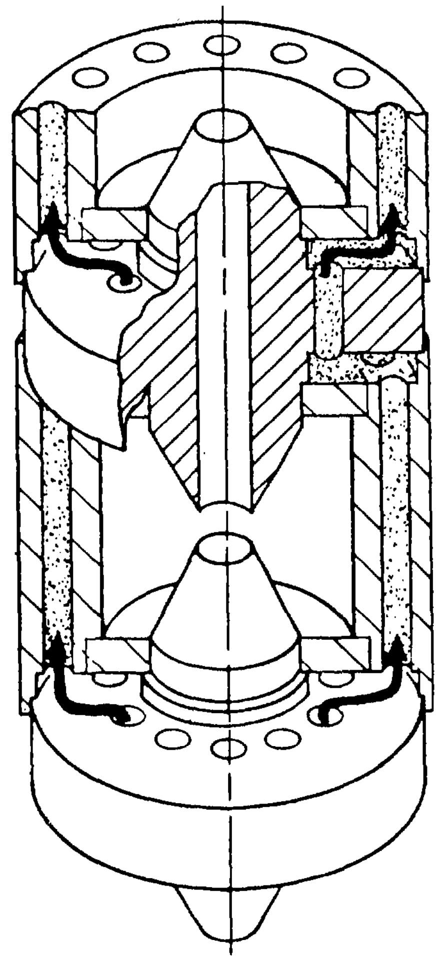

Fig. 10. New cavity structure (VKS-8274 JPL)

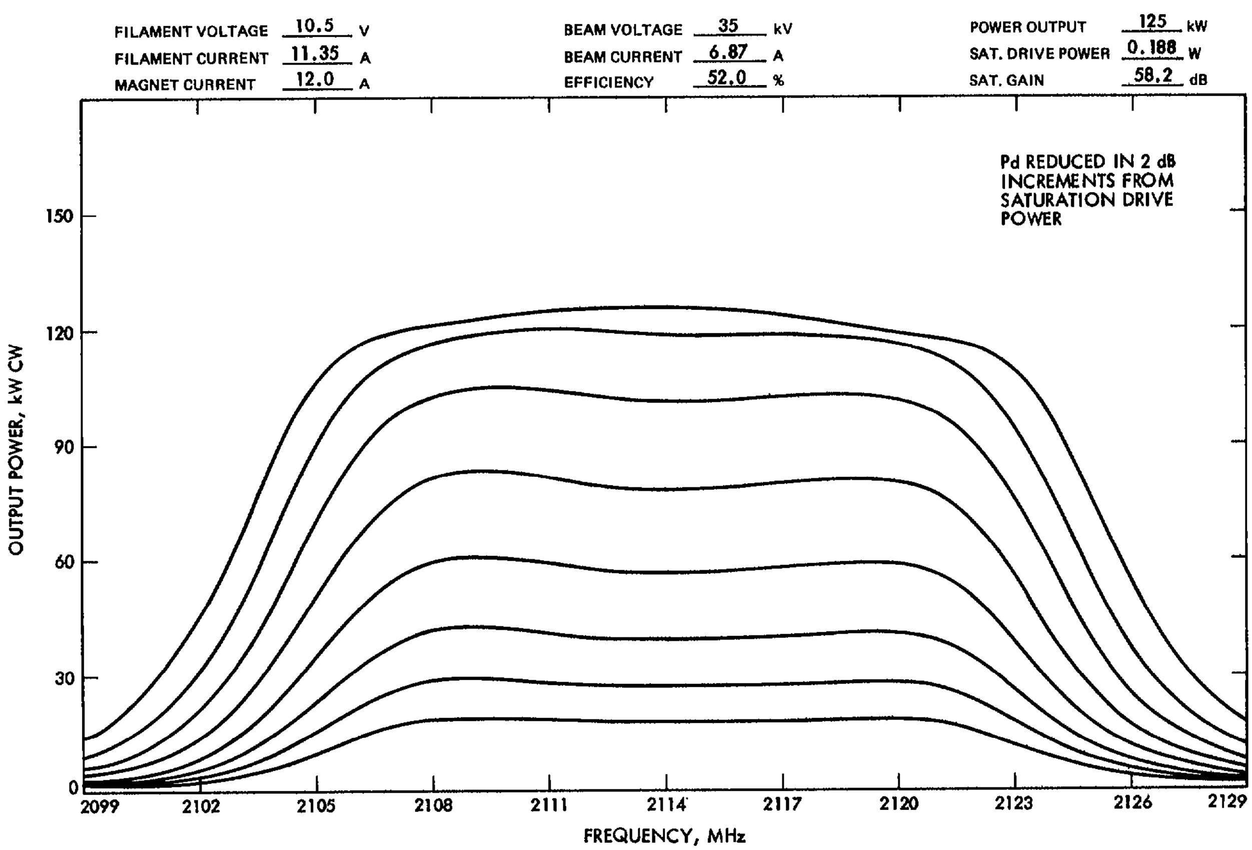

Fig. 11. Output power vs frequency

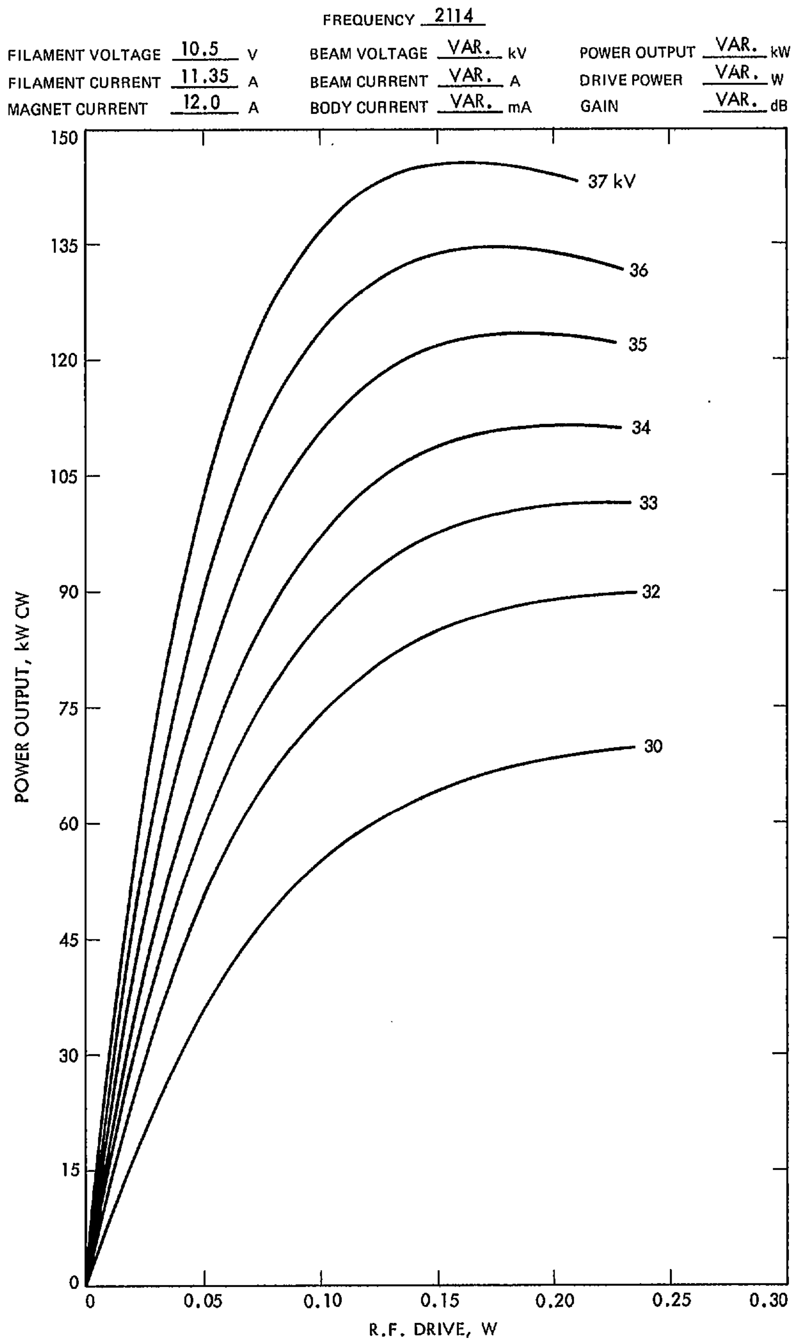

Fig. 12. Output power vs drive power

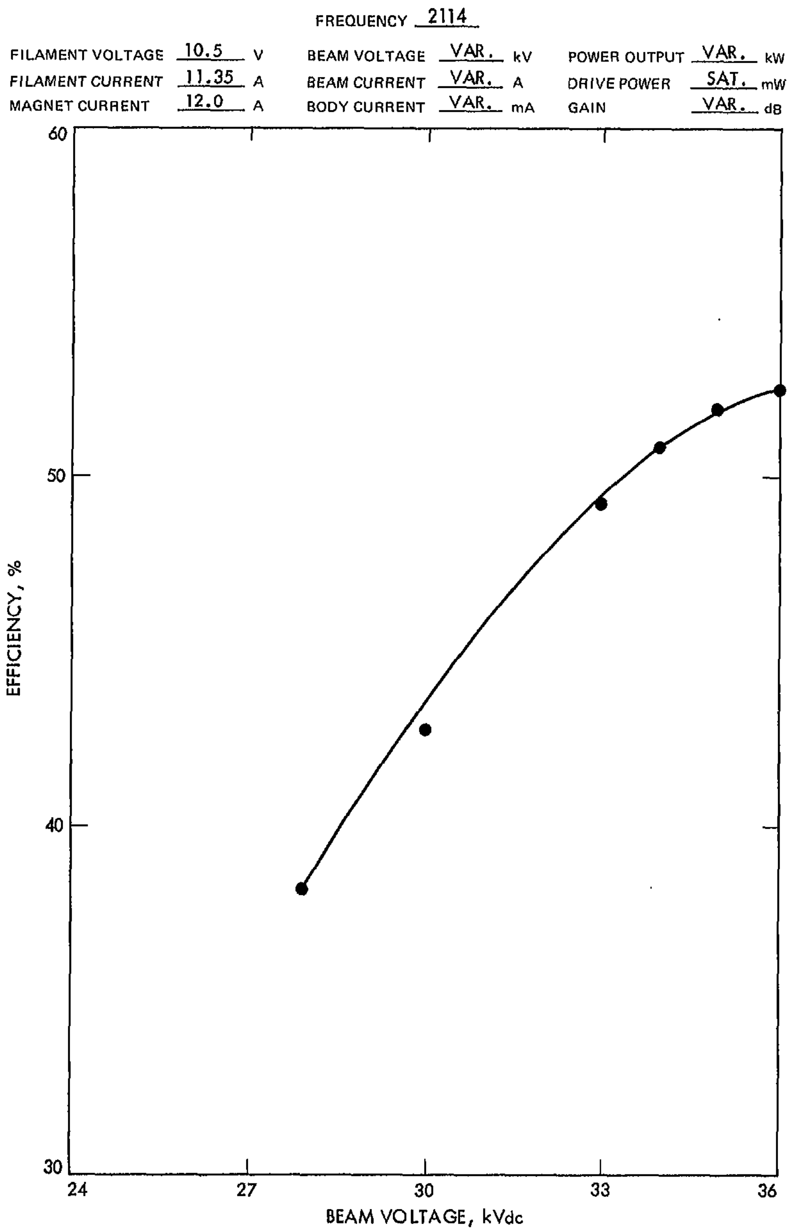

Fig. 13. VKS-8274 efficiency